Organic & Biomolecular Chemistry

ROYAL SOCIETY OF CHEMISTRY

PAPER

View Article Online
View Journal | View Issue

Check for updates

Cite this: *Org. Biomol. Chem.*, 2025, **23**, 8914

Direct synthesis of 2,3-dihydroperimidine derivatives *via* dehydrogenative C–N coupling using a recyclable Fe catalyst

Vageesh M,† Sandra Shabu† and Raju Dey *

Received 20th June 2025,
Accepted 19th August 2025

DOI: 10.1039/d5ob01009h

rsc.li/obc

We report here an efficient and sustainable protocol for the direct synthesis of 2,3-dihydroperimidine derivatives *via* dehydrogenative C–N coupling, utilizing a recyclable Fe single-atom catalyst supported on nitrogen-doped carbon (Fe_1–N–C). The catalyst was synthesized by encapsulating ferrocene within the ZIF-8 framework, followed by pyrolysis. The catalyst exhibited excellent activity, stability, and recyclability, facilitating the transformation of diverse primary alcohols, including aryl/heteroaryl methanol and aliphatic alcohols, into the desired products in moderate to good yields. To delineate the mechanism, several control experiments were performed, revealing the formation of aldehyde as the intermediate, which subsequently underwent annulation with naphthalene-1,8-diamine. Additionally, the gram-scale synthesis further showcased the versatility of the catalyst as well as the protocol.

Introduction

Nitrogen-containing heterocyclic molecules are ubiquitous and play a significant role as pharmaceuticals,[1] agrochemicals,[2] and biologically active products.[3] Their biological activity, coupled with their ability to readily protonate or deprotonate and to form various weak interactions such as H-bonding and dipole–dipole interactions, makes them indispensable in various fields of organic and pharmaceutical chemistry.[4] Among various nitrogen-containing heterocycles, perimidines stand out as a class of scaffolds that are renowned for their multifunctional properties.[5] Perimidine derivatives have been extensively employed as ligands for catalysts,[6] conducting polymers,[7] dyes,[8] photosensors as well as supramolecular self-assembly,[9] and corrosion inhibitors.[10] They exhibit a wide range of biological activities, including antioxidant,[11] anticancer,[12] antimicrobial,[13] anti-inflammatory,[14] and acetylcholinesterase inhibitory activities (Fig. 1).[15]

Perimidine derivatives are conventionally synthesized through a condensation reaction between 1,8-diaminonaphthalene and aldehydes, using mineral acids or Lewis acids as catalysts.[16] Moreover, the synthesis of 2,3-dihydroperimidine derivatives has been effectively facilitated by employing SiO_2 and zeolite-based catalytic systems.[17] However, most of the protocols are associated with the generation of stoichiometric waste, harsh reaction conditions, and low atom economy. In recent times, due to alarming environmental concerns, more emphasis has been placed on sustainable organic synthesis. Over the past decade, acceptorless dehydrogenation of alcohols has emerged as a sustainable and atom-economical strategy for the construction of C–C and C–heteroatom bonds and the synthesis of heterocycles with water and hydrogen being the sole byproducts.[18] Thus, numerous research groups are engaged in the development of highly active and selective homogeneous as well as heterogeneous catalyst systems for acceptorless dehydrogenation.[19] To meet the growing demand for an active, robust, and inexpensive catalyst, single-atom catalysts (SACs) have emerged as the new frontier in catalytic chemical processes.[20] Not only do they exhibit excellent activity, selectivity, and tunability, but they also have tra-

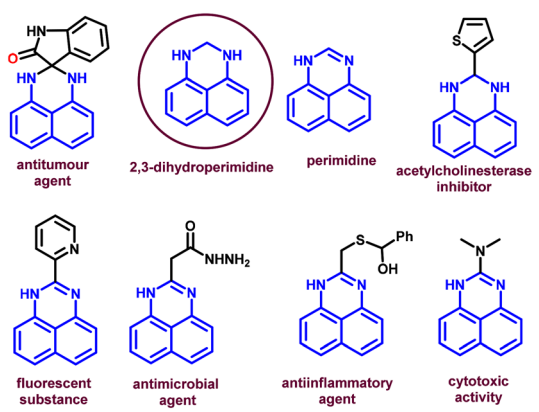

Fig. 1 Representative important perimidine derivatives.

Department of Chemistry, National Institute of Technology Calicut, 673601 Kozhikode, Kerala, India. E-mail: rajudey@nitc.ac.in
†These authors have contributed equally to this work.

ditional heterogeneous characteristics like stability, recyclability, and easy separation from the product.[21] SACs offer maximum atom utility, efficiency of the catalytic centers, and stability and can function under diverse reaction conditions.[22]

The synthesis of 2,3-dihydroperimidine derivatives *via* acceptorless dehydrogenation of alcohols, followed by annulation with naphthalene-1,8-diamine, is known in the literature but not widely explored. Ramesh *et al.* developed palladium(II) complexes as catalysts for the synthesis of 2,3-dihydro-1*H*-perimidine.[23]

Recently, Srimani and coworkers accomplished the synthesis of 2,3-dihydro-1*H*-perimidine derivatives by utilizing a homogeneous Co-complex[24] and a Mn complex[25] as a catalytic system (Scheme 1). Furthermore, Dateer *et al.* reported the synthesis of perimidine derivatives using single-phase δ-MnO_2 NPs.[26] Wang and team achieved the same transformation utilizing recyclable mesoporous silica-supported iridium and ruthenium catalysts.[27] During our thorough literature survey, we didn't come across any 3d transition metal heterogeneous catalyst for the synthesis of 2,3-dihydro-1*H*-perimidine derivatives *via* acceptorless dehydrogenative coupling. Hence, as a part of a continuing program to explore the novel applications of acceptorless dehydrogenation,[28] we explore here the synthesis of 2,3-dihydro-1*H*-perimidine derivatives utilizing an earth-abundant, inexpensive, and environmentally benign Fe-based catalyst system. Previously, our group developed an iron single-atom catalyst on nitrogen-doped carbon (Fe_1–N–C) for the direct formation of the Csp^3–S bond *via* the borrowing hydrogen strategy using alcohols as the alkylating agent.[29] The catalyst was synthesized using a ferrocene encapsulated zeolitic imidazole framework (Fc@ZIF-8) as the precursor, which, on pyrolysis at 900 °C, leads to the reduction of ZnO and evaporation of Zn, increasing the surface area and encasing Fe atoms into the Zn vacancies.[30]

Results and discussion

The catalyst precursor Fc@ZIF-8 was synthesized using readily available and inexpensive precursors ferrocene (Fc), $Zn(NO_3)_2$, and 2-methylimidazole. Furthermore, the former was pyrolyzed under an argon atmosphere at 900 °C to obtain the desired catalyst Fe_1–N–C. The synthesized Fe_1–N–C was characterized by EXAFS, XPS, HR-TEM, XRD, ICP-OES, Raman spectroscopy, *etc*. The reusability of the catalyst was tested for the current protocol, and it could be recycled 5 times without appreciably affecting the catalyst activity (Fig. 3).

The XRD patterns of the catalysts presented only characteristic peaks corresponding to graphitic carbon, ranging from 20 to 30° (002) and 40 to 50° (101), and no signals corresponding to crystalline metal or metal oxide were observed (Fig. S4).[29,31] The presence of iron single atoms (encircled in red) was determined by HR-TEM (Fig. 2a and b). EXAFS measurement of the catalyst further validated the single atomic nature of iron in the catalyst (Fig. 2c). In the EXAFS spectrum, a peak at a radial distance of ~1.4 Å corresponding to the Fe–N bond was observed. However, Fe–Fe interaction peaks at ~2.1 Å, 3.7 Å and 4.4 Å were found to be absent in the EXAFS signal of Fe_1–N–C, further confirming the single atomic nature of iron in the catalyst. To obtain insights into the electronic properties and oxidation state of the surface species present in the catalyst, XPS analysis was carried out. The XPS spectrum of the nitrogen region (Fig. 2d) revealed the presence of four different nitrogen species *i.e.* pyridinic N (398.4 eV), pyrrolic N (400.1 eV), graphitic N (401.2 eV), and oxidized nitrogen species (402.9 eV).[29] It was observed that the integrated peak

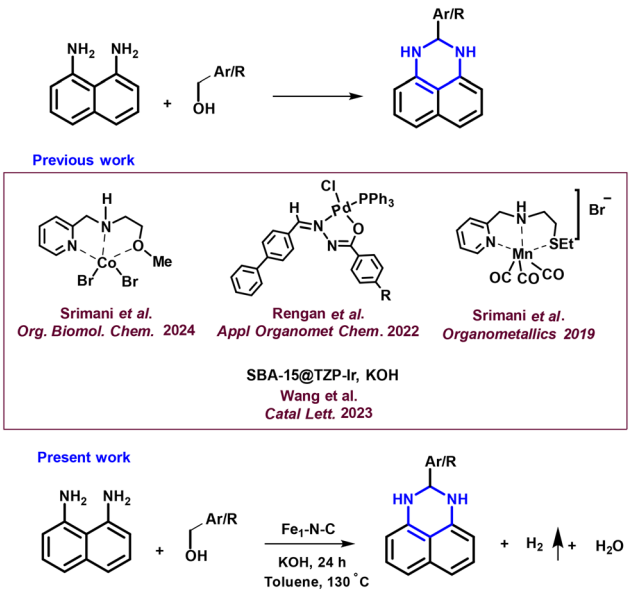

Scheme 1 State of the art in the synthesis of 2,3-dihydro-1*H*-perimidine derivatives *via* acceptorless dehydrogenative annulation.

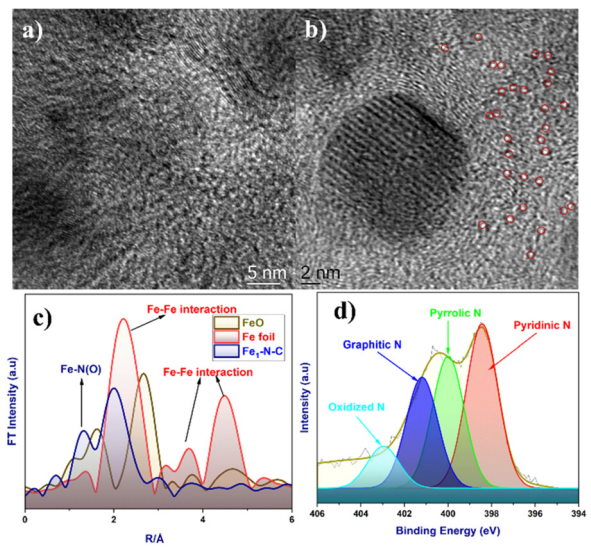

Fig. 2 (a) HR-TEM image of Fe_1–N–C, (b) magnified HR-TEM image of Fe_1–N–C with Fe single atoms encircled in red, (c) EXAFS spectrum of Fe_1–N–C, Fe metal and FeO, (d) XPS spectrum of N in Fe_1–N–C.

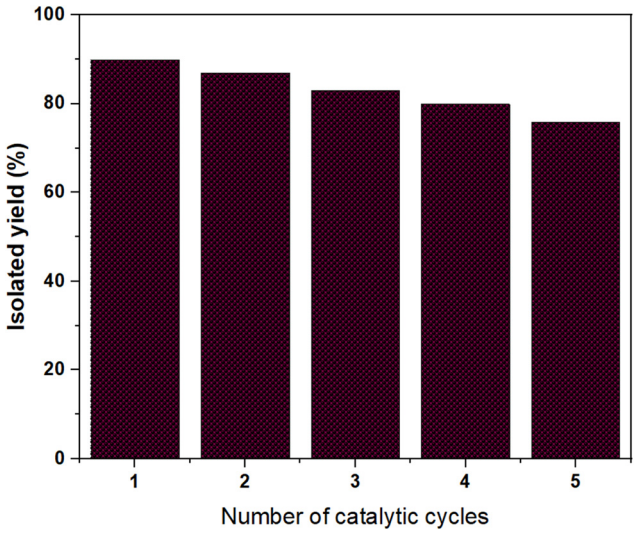

Fig. 3 Recyclability test carried out using benzyl alcohol and naphthalene-1,8-diamine under standard reaction conditions.

area of pyridinic type N was higher when compared with others and is presumed to be the anchor sites to the Fe atoms. The actual Fe loading in the catalyst was determined by ICP-OES and found to be 0.65 wt%. Furthermore, HAADF-elemental mapping provided the elemental distribution in the catalyst (Fig. S5, SI).

Following detailed characterization of the catalyst, we investigated the catalytic activity of the catalyst in the acceptorless dehydrogenative coupling between 4-methylbenzyl alcohol and naphthalene-1,8-diamine as the model substrates. Various crucial reaction parameters like catalyst, solvent, reaction time, and temperature were varied to achieve the optimal reaction conditions (Table 1 and Table S1, SI).

A complete conversion into the product with 80% isolated yield was achieved when 0.5 mmol of naphthalene-1,8-diamine, 1 mmol of 4-methylbenzyl alcohol, 1 mmol of KOH, and 5 mg of Fe_1–N–C catalyst were stirred in toluene medium at 130 °C for 24 h (Table 1, entry 2). A reduction in the reaction temperature and time resulted in a significant reduction in the yield of 2-tolyl-2,3-dihydro-1*H*-perimidine, indicating the critical dependence of product formation on the optimized temperature and time (Table 1, entries 3 and 4). The base KOH was indispensable for the current protocol, and carrying out the reaction without it (Table 1, entry 5) or replacing it with milder bases like K_2CO_3 (Table 1, entry 10) resulted in the recovery of the limiting reagent, naphthalene-1,8-diamine, without product formation. As expected, the reaction didn't proceed efficiently in the absence of the catalyst, leaving the majority of the reactants unreacted (Table 1, entry 1). Similarly, no promising results were observed when the catalyst precursors ferrocene, $Zn(NO_3)_2$, and Fc@ZIF-8 were used as the catalyst (Table 1, entries 6–8). These outcomes emphasize the critical role of the Fe_1–N–C catalyst in the current protocol. The reaction was not feasible in polar solvents, including DMF (Table 1, entry 9), DMSO, and water (Table S1, entries 11 and 12).

To demonstrate the versatility of the current protocol, we expanded the substrate scope by employing a range of benzyl alcohols and aliphatic alcohols. It was observed that the reaction was uniform irrespective of the functional group present. Benzyl alcohol with electron-donating groups at the *para* position, such as 4-Me, 4-OMe, and 4-^{i}pr, furnished the desired 2-phenyl-2,3-dihydro-1*H*-perimidine derivatives in good yields (Table 2, entries 3b–3d). A similar observation was made when 2-aminobenzyl alcohol was employed as the substrate (Table 2, entry 3e). Furthermore, the trend continued with halogen-substituted benzyl alcohols, and 2-phenyl-2,3-dihydro-1*H*-perimidine derivatives were obtained in moderate to good yields

Table 1 Optimization of reaction conditions[a]

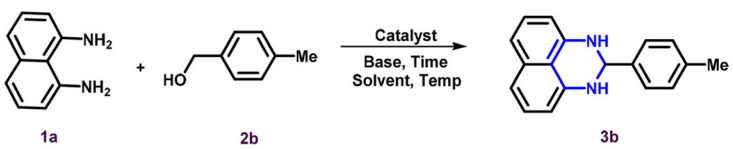

1a 2b 3b

Entry	Catalyst	Solvent	Temperature[c] (°C)	Base	Time (h)	Yield[b] (%)
1	—	Toluene	130	KOH	24	10
2	Fe_1–N–C	Toluene	130	KOH	24	80
3	Fe_1–N–C	Toluene	110	KOH	24	48
4	Fe_1–N–C	Toluene	130	KOH	16	59
5	Fe_1–N–C	Toluene	130	—	24	—
6	Ferrocene[d]	Toluene	130	KOH	24	9
7	$Zn(NO_3)_2$	Toluene	130	KOH	24	7
8	Fc@ZIF-8	Toluene	130	KOH	24	19
9	Fe_1–N–C	DMF	130	KOH	24	—
10	Fe_1–N–C	Toluene	130	K_2CO_3	24	—

[a] Reaction conditions: 4-methylbenzyl alcohol (1 mmol), naphthalene-1,8-diamine (0.5 mmol), catalyst (5 mg), solvent (2 mL), and base (1 mmol) were stirred under an argon atmosphere for the required time using a preheated heating block. [b] Yield refers to isolated yield. [c] Heating block temperature. [d] Catalyst amount equivalent to 0.6 wt% of Fe was used.

Table 2 Substrate scope[a,b]

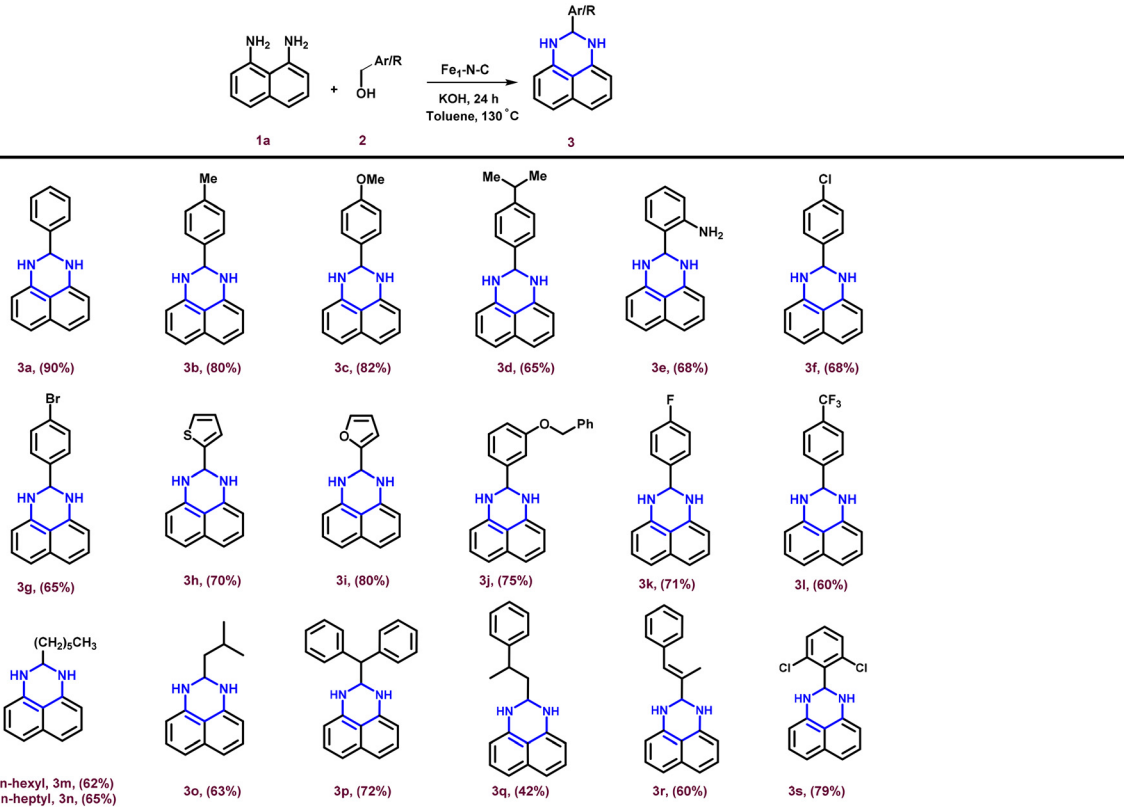

[a] Reaction conditions: alcohol (1 mmol), naphthalene-1,8-diamine (0.5 mmol), Fe_1–N–C (5 mg, Fe loading 0.65 wt%), toluene (2 mL), and KOH (1 mmol) were stirred under an argon atmosphere for 24 h on a preheated heating block maintained at 130 °C. [b] Yield refers to isolated yield of pure compounds characterized by ^{1}H, ^{13}C NMR and mass spectroscopy.

(Table 2, entries 3f, 3g, and 3k). Notably, the 4-CF_3 functional group also furnished the desired perimidine derivative in good yield (Table 2, entry 3l). The protocol scope was further extended beyond benzyl alcohols, heteroaryl primary alcohols like thiophen-2-yl methanol (Table 2, entry 3h), furfural alcohol (Table 2, entry 3i), and aliphatic alcohols including heptanol, octanol, isoamyl alcohol, 3-phenyl butanol and diphenyl methanol all of which furnished the corresponding 2,3-dihydroperimidine derivatives in gratifying yields (Table 2, entries 3n–3q). Hydrogen labile groups, such as *O*-benzyl, remained intact under the present reaction protocol (Table 2, entry 3j). Moreover, when α-*trans* methyl cinnamyl alcohol was employed, the reaction proceeded selectively at the terminal carbon with 60% yield of the desired product (Table 2, entry 3r). Furthermore, when 2,6-dichlorobenzyl alcohol was deployed, the corresponding product was obtained in good yield (Table 2, entry 3s). In addition, to check the large-scale utility of the protocol and the catalyst, a gram-scale synthesis was performed by employing naphthalene-1,8-diamine and thiophenyl-1-methanol under the standard reaction conditions. To our delight, we were able to isolate the corresponding 2,3-dihydroperimidine derivatives containing the thiophene moiety, a potent acetylcholinesterase inhibitor, in 52% yield (Scheme 2).

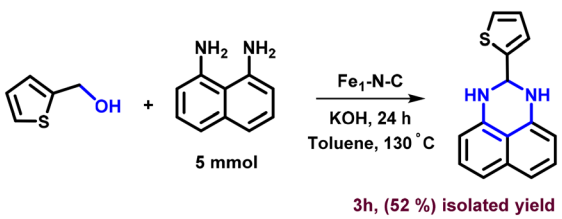

Scheme 2 Gram-scale synthesis of 2,3-dihydro-1*H*-perimidine derivatives containing the thiophene moiety, a potent acetylcholinesterase inhibitor.

To gain mechanistic insights into the synthesis of 2,3-dihydroperimidine derivatives, a series of control experiments were carried out and are summarized in Fig. 4. When the reaction was carried out under the standard reaction conditions by employing only 4-methylbenzyl alcohol along with the catalyst Fe_1–N–C, it led to the formation of 4-methylbenzaldehyde (Fig. 4, eqn (i)) *via* acceptorless dehydrogenation with the liberation of hydrogen gas, which was qualitatively detected using gas chromatography (Fig. S6, SI). Furthermore, when the reaction was carried out using 4-methylbenzaldehyde instead of 4-methylbenzyl alcohol, under the standard reaction conditions, we obtained the desired 2-tolyl-2,3-dihydro-1*H*-perimi-

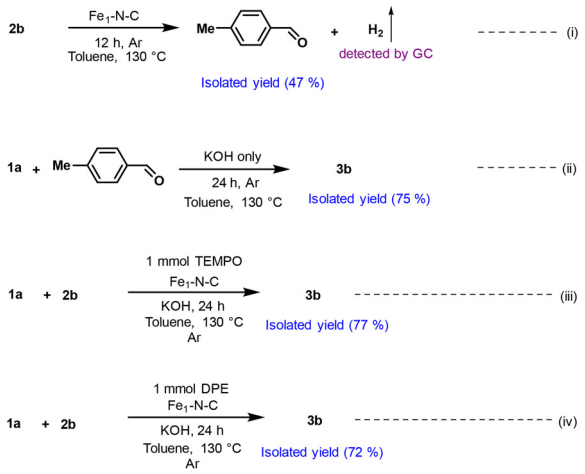

Fig. 4 Control experiments. Reaction conditions: 4-methylbenzyl alcohol/4-methylbenzaldehyde (1 mmol), naphthalene-1,8-diamine (0.5 mmol, for reaction ii–iv), Fe_1–N–C (5 mg, Fe loading 0.65 wt%), toluene (2 mL), and KOH (1 mmol) were stirred under an argon atmosphere for 24 h using a preheated heating block. For reactions iii–iv, 1 mmol radical scavengers were used.

dine in 75% isolated yield, confirming that aldehyde is the intermediate formed during the course of the reaction (Fig. 4, eqn (ii)). To eliminate the possibility of a radical pathway, a radical scavenging test was performed using 2,2,6,6-tetramethylpiperidinyloxy (TEMPO) and 1,1-diphenylethylene (DPE). The reaction proceeded smoothly even in the presence of radical scavengers, furnishing the desired product with 77% and 72% yields, respectively (Fig. 4, eqn (iii) and (iv)).

Based on these experimental findings, a plausible reaction mechanism was proposed as shown in Scheme 3, where at the beginning, alcohol undergoes an Fe_1–N–C catalyzed acceptorless dehydrogenation to give the corresponding aldehyde. The aldehyde subsequently undergoes nucleophilic attack by naphthalene-1,8-diamine, followed by base-catalyzed condensation, leading to the formation of the desired 2,3-dihydro-1*H*-perimidine derivative as the final product.

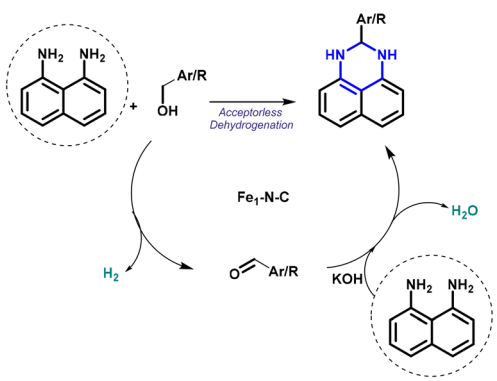

Scheme 3 Plausible reaction mechanism.

Conclusions

In conclusion, the synthesis of 2,3-dihydro-1*H*-perimidine derivatives has been demonstrated by employing an iron single atom on nitrogen-doped carbon (Fe_1–N–C) as a catalyst *via* acceptorless alcohol dehydrogenation. The catalyst Fe_1–N–C displayed good activity, stability, and recyclability, and was synthesized using inexpensive precursors *via* high-temperature pyrolysis and sacrificial template strategies. The catalyst was characterized by various analytical and spectroscopic techniques, including HR-TEM and EXAFS measurement, which confirm the well-dispersed Fe-single atom on the nitrogen-doped carbon (N–C) support. The versatility of the protocol and catalyst was validated using a wide range of substrates, including benzyl alcohols containing electron-donating, electron-withdrawing, halogen, and hydrogenation-labile substituents, heteroaryl methanols, and aliphatic alcohols. A wide array of functional groups was tolerated, and the corresponding 2,3-dihydro-1*H*-perimidine was furnished in moderate to good yields. Control experiments suggested that the reaction proceeds *via* the formation of an aldehyde intermediate, followed by annulation with naphthalene-1,8-diamine.

Conflicts of interest

The authors declare no conflict of interest.

Data availability

The data that support the findings of this study are available within the article and the SI. See DOI: **https://doi.org/10.1039/d5ob01009h**.

The supporting information includes general information, experimental procedures, material characterization and analytical data of compounds in Table 2.

Acknowledgements

R. D. acknowledges the National Institute of Technology Calicut for research funding. V. M. is thankful to NIT Calicut for his fellowship. The DST-FIST supported HRMS facility at the Department of Chemistry, NIT Calicut, is acknowledged for high-resolution mass spectrometric measurement. The authors are grateful to CMC-NIT Calicut for providing the NMR facility. The R-XAS facility at the Sophisticated Instrumentation Centre, IIT Indore, is acknowledged for EXAFS measurement.

References

1 M. M. Heravi and V. Zadsirjan, *RSC Adv.*, 2020, **10**, 44247–44311.
2 V. V. Chernyshov, I. I. Popadyuk, O. I. Yarovaya and N. F. Salakhutdinov, *Top. Curr. Chem.*, 2022, **380**, 42.

3 E. A. Bakhite, A. A. Abd-Ella, M. E. A. El. Sayed and S. A. A. Abdel-Raheem, *J. Agric. Food Chem.*, 2014, **62**, 9982–9986.
4 C. M. Marshall, J. G. Federice, C. N. Bell, P. B. Cox and J. T. Njardson, *J. Med. Chem.*, 2024, **67**(14), 11622–11655.
5 (*a*) M. Azam, I. Warad, S. I. Al-Resayes, N. Alzaqri, M. R. Khan, R. Pallepogu, S. Dwivedi, J. Musarrat and M. Shakir, *J. Mol. Struct.*, 2013, **1047**, 48–54; (*b*) M. Azam, I. Warad, S. I. Al-Resayes, M. Zahin, I. Ahmad and M. Shakir, *Z. Anorg. Allg. Chem.*, 2012, **638**, 881–886; (*c*) F. A. Bassyouni, S. M. Abu-Bakr, K. H. Hegab, W. El-Eraky, A. A. El-Beih and M. E. A. Rehim, *Res. Chem. Intermed.*, 2012, **38**, 1527–1528; (*d*) M. F. Braña, M. Garrido, M. L. Lopez-Rodriguez, M. J. Morcillo, Y. Alvarez, Y. Valladares and G. Klebe, *Eur. J. Med. Chem.*, 1990, **25**, 209–215; (*e*) B. Stefańska, M. Dzieduszycka, M. M. Bontemps-Gracz, E. Borowski, S. Martelli, R. Supino, G. Pratesi, M. A. de Cesare, F. Zunino, H. Kuśnierczyk and C. Radzikowski, *J. Med. Chem.*, 1999, **42**, 3494–3501; (*f*) X. Bu, W. L. Deady, G. J. Finlay, B. C. Baguley and W. A. Denny, *J. Med. Chem.*, 2001, **44**, 2004–2014.
6 A. F. Pozharskii, A. V. Gulevskaya, R. M. Claramunt, I. Alkorta and J. Elguero, *Russ. Chem. Rev.*, 2020, **89**, 1204.
7 (*a*) M. Czichy, H. Zhylitskaya, P. Zassowski, M. Navakouski, P. Chulkin, P. Janasik, M. Lapkowski and M. Stepien, *J. Phys. Chem. C*, 2020, **124**, 14350–14362; (*b*) P. Janasik, P. Chulkin, M. Czichy and M. Lapkowski, *Sci. Rep.*, 2024, **14**, 21027.
8 (*a*) R. A. Jeffreys, *J. Chem. Soc.*, 1955, 2394–2397; (*b*) S. Sahiba, N. Nusrat and S. Agarwal, *Top. Curr. Chem.*, 2020, **378**, 44.
9 S.-Y. Fan, H.-T. Xu, Q.-G. Li, D.-M. Fang, W.-H. Yu, S.-K. Xiang, P. Hu, K.-Q. Zhao, C. Feng and B.-Q. Wang, *Liq. Cryst.*, 2020, **47**, 1041–1054.
10 Q. Ma, J. Cai, S. Mu, H. Zhang, K. Liu, J. Liu and J. Hong, *Coatings*, 2023, **13**, 73.
11 K. Padmavathy, K. GokulaKrishnan, C. U. Kumar, P. Sutha, R. Sivaramakarthikeyan and C. Ramalingan, *ChemistrySelect*, 2018, **3**, 5965–5974.
12 H. A. Eldeab and A. F. Eweas, *J. Heterocycl. Chem.*, 2018, **55**, 431.
13 T. A. Farghaly, M. A. Abdallah and Z. A. Muhammad, *Res. Chem. Intermed.*, 2015, **41**, 3937–3947.
14 F. A. Bassyouni, S. M. Abu-Bakr, K. H. Hegab, W. El-Eraky, A. A. El Beih and M. E. A. Rehim, *Res. Chem. Intermed.*, 2012, **38**, 1527–1550.
15 M. Alam and D.-U. Lee, *Comput. Biol. Chem.*, 2016, **64**, 185–201.
16 (*a*) M. M. Belmonte, E. C. Escudero-Adán, J. Benet-Buchholz, R. M. Haak and A. W. Kleij, *Eur. J. Org. Chem.*, 2010, 4823–4831; (*b*) N. A. Harry, R. M. Cherian, S. Radhika and G. Anilkumar, *Tetrahedron Lett.*, 2019, **60**, 150946; (*c*) K. Bahrami and S. Saleh, *Synth. React. Inorg., Met.-Org., Nano-Met. Chem.*, 2016, **46**, 852–856; (*d*) M. Kalhor and N. Khodaparast, *Res. Chem. Intermed.*, 2015, **41**, 3235–3242; (*e*) A. Bamoniri, B. F. Mirjalili and S. Saleh, *RSC Adv.*, 2018, **8**, 6178.
17 (*a*) H. Alinezhad, A. Ahmadi and P. Hajiabbasi, *J. Chem. Sci.*, 2019, **131**, 34; (*b*) M. Kalhor, F. Rezaee-Baroonaghi, A. Dadras and Z. Zarnegar, *Appl. Organomet. Chem.*, 2019, **33**, 4784; (*c*) M. Kalhor, Z. Zarnegar, F. Janghorban and S. A. Mirshokraei, *Res. Chem. Intermed.*, 2020, **46**, 821–836; (*d*) P. B. Shelke, S. N. Mali, H. K. Chaudhari and A. P. Pratap, *J. Heterocycl. Chem.*, 2019, **56**, 3048.
18 (*a*) M. Maji, D. Panja, I. Borthakur and S. Kundu, *Org. Chem. Front.*, 2021, **8**, 2673–2709; (*b*) N. Hofmann and K. C. Hultzsch, *Eur. J. Org. Chem.*, 2021, 6206–6223.
19 K. Wang, J. Horlyck, N. An and A. Voutchkova-Kostal, *Green Chem.*, 2024, **26**, 3546–3564.
20 L. Jiao and H.-L. Jiang, *Chem*, 2019, **5**, 786–804.
21 X.-F. Yang, A. Wang, B. Qiao, J. U. N. Li, J. Liu and T. Zhang, *Acc. Chem. Res.*, 2013, **46**, 1740–1748.
22 R. Lang, X. Du, Y. Huang, X. Jiang, Q. Zhang, Y. Guo, K. Liu, B. Qiao, A. Wang and T. Zhang, *Chem. Rev.*, 2020, **120**, 11986–12043.
23 S. S. Clinton, R. Ramesh and J. G. Małecki, *Appl. Organomet. Chem.*, 2022, **36**, e6708.
24 D. Pal, R. Sarmah, A. Mondal, I. Mallick and D. Srimani, *Org. Biomol. Chem.*, 2024, **22**, 8602–8607.
25 K. Das, A. Mondal, D. Pal, H. K. Srivastava and D. Srimani, *Organometallics*, 2019, **38**, 1815–1825.
26 R. Nandini, R. Thrilokraj, U. A. Kshirsagar, R. V. Hegde, A. Ghosh, S. A. Patil, J. G. Malecki and R. B. Dateer, *New J. Chem.*, 2024, **48**, 1327–1335.
27 B. Zhang, J. Li, H. Zhu, X.-F. Xia and D. Wang, *Catal. Lett.*, 2023, **153**, 2388–2397.
28 (*a*) H. P., V. M. and R. Dey, *RSC Adv.*, 2024, **14**, 10761; (*b*) V. M., O. Patil, H. P. and R. Dey, *Synlett*, 2024, 2496; (*c*) H. P., M. Tomasini, A. Poater and R. Dey, *ChemistrySelect*, 2024, **9**, e202400468.
29 V. M., H. P., P. A. Bhobe and R. Dey, *Org. Biomol. Chem.*, 2024, **13**, e202400032.
30 (*a*) L. Jiao, J. Zhu, Y. Zhang, W. Yang, S. Zhou, A. Li and H. L. Jiang, *J. Am. Chem. Soc.*, 2021, **143**, 19417–19424; (*b*) K. Sun, H. Shan, H. Neumann, G. P. Lu and M. Beller, *Nat. Commun.*, 2022, **13**, 1848.
31 J. Wang, G. Han, L. Wang, L. Du, G. Chen, Y. Gao, Y. Ma, C. Du, X. Cheng, P. Zuo and G. Yin, *Small*, 2018, **14**, 1704282.